Title: Targeting host deoxycytidine kinase attenuates *Staphylococcus aureus* virulence

Authors: Volker Winstel[1,2]*, Evan R. Abt[3], Caius G. Radu[3]

Affiliations:

[1] Research Group Pathogenesis of Bacterial Infections; TWINCORE, Centre for Experimental and Clinical Infection Research, a joint venture between the Hannover Medical School and the Helmholtz Centre for Infection Research, Hannover, Germany

[2] Institute of Medical Microbiology and Hospital Epidemiology, Hannover Medical School, Hannover, Germany

[3] Department of Molecular and Medical Pharmacology, David Geffen School of Medicine, UCLA, Los Angeles, United States of America

* Address **correspondence** to Volker Winstel: winstel.volker@mh-hannover.de

Institute of Medical Microbiology and Hospital Epidemiology, Hannover Medical School
Carl-Neuberg-Str. 1, 30625 Hannover, Germany
Phone: +49 511 22002 7220 / Fax: +49 511 22002 7186

Abstract

Host-directed therapy (HDT) is an emerging approach to overcome antimicrobial resistance in pathogenic microorganisms. Specifically, HDT targets host-encoded factors required for pathogen replication and survival without interfering with microbial growth or metabolism, thereby eliminating the risk of resistance development. By applying HDT and a drug repurposing approach, we demonstrate that (*R*)-DI-87, a clinical-stage anti-cancer drug and potent inhibitor of mammalian deoxycytidine kinase (dCK), attenuates the virulence of antibiotic-resistant *Staphylococcus aureus* in a mouse model of bloodstream infection. Mechanistically, (*R*)-DI-87 shields phagocytes from staphylococcal death-effector deoxyribonucleosides that target dCK and the mammalian purine salvage pathway-apoptosis axis. In this manner, (*R*)-DI-87-mediated protection of immune cells amplifies macrophage infiltration into deep-seated abscesses, a phenomenon coupled with enhanced pathogen control, ameliorated immunopathology, and reduced disease severity. Thus, pharmaceutical blockade of dCK represents an advanced anti-infective intervention strategy against which staphylococci cannot develop resistance and may help to fight fatal infectious diseases in hospitalized patients.

Introduction

Hospital- and community-acquired infections caused by antibiotic-resistant bacterial pathogens represent a global public health threat (Wenzel, 2007; GBD 2019 Antimicrobial Resistance Collaborators, 2022a; b). Specifically, infections caused by multidrug-resistant microbes are often associated with increased morbidity and mortality, as compared to infections caused by antibiotic-sensitive strains (Klevens et al., 2008; Yaw et al., 2014; GBD 2019 Antimicrobial Resistance Collaborators, 2022a; b). In addition, the pathology of various bacterial infections includes multifactorial manipulation of host multicellular assemblies that enable pathogen replication, dissemination of disease, and adaptation to new hosts (Foster, 2005; Finlay and McFadden, 2006; Okumura and Nizet, 2014; Thammavongsa et al., 2015). Thus, prevention and therapy of such infections represent a major challenge in clinical practice and frequently require administering last-resort antibiotics such as vancomycin, linezolid, or colistin (Chambers and Deleo, 2009; McKenna, 2013; Tong et al., 2015). However, many clinically relevant pathogens have already developed resistance-mechanisms against many of these drugs thereby rendering antibiotic therapy of appropriate infections often ineffective (Meka and Gold, 2004; Chambers and Deleo, 2009; GBD 2019 Antimicrobial Resistance Collaborators, 2022a). Moreover, the rapid exchange of antibiotic resistance genes via horizontal gene transfer events, along with the large-scale usage of antimicrobials in hospitals and in the animal industry, continuously triggers the emergence of new drug-resistant and globally spreading bacterial clones, highlighting the desperate need for novel treatment options to fight infectious diseases in human or animal hosts (Chambers and Deleo, 2009; Nubel, 2016; Jian et al., 2021).

Antibiotic-resistant bacteria are frequently associated with local and life-threatening infections in both, hospital environments and in the general community. Of particular concern are Mycobacteria, certain Gram-negative as well as Gram-positive bacteria including *Staphylococcus aureus*, a notorious pathogen that colonizes approximately 30% of the human population (Lowy, 1998; Kuehnert et al., 2006; Lee et al., 2018). *S. aureus* causes skin and soft tissue infections and is a widespread cause of endocarditis, septic arthritis, osteomyelitis, bacteremia, and sepsis (Lowy, 1998; Fridkin et al., 2005; Klevens et al., 2007). Moreover, this microbe triggers toxic shock syndrome, food poisoning, ventilator-associated pneumonia, and associated infections of the respiratory tract (Lowy, 1998; Lee et al., 2018; Torres et al., 2021). Nonetheless, a hallmark of staphylococcal disease is the formation of suppurative abscesses, where *S. aureus* provokes inflammatory responses that attract neutrophils, macrophages, and other immune cells to the site of the infection (Lowy, 1998; Cheng et al., 2011; Spaan et al., 2013). Abscess formation is further accompanied by liquefaction necrosis, the release of purulent exudates into circulating body fluids, and several defensive host responses designed to limit staphylococcal replication and spread (Cheng et al., 2011). For example, staphylococcal invasion of host tissues and abscess formation includes deposition of structural fibrin clusters, which shield

healthy tissues from disseminating staphylococci (Cheng et al., 2011). Moreover, neutrophils combat *S. aureus* by powerful mechanisms which involve phagocytosis, generation of reactive oxygen species, and the formation of neutrophil extracellular traps (NETs) (Spaan et al., 2013). NETs represent an extracellular matrix composed of nuclear and mitochondrial DNA spiked with antimicrobial peptides, cell-specific proteases, and granular proteins that together ensnare and kill microbial invaders (Brinkmann et al., 2004). However, *S. aureus* rapidly evades NET-mediated killing due to the secretion of a potent nuclease (Nuc) capable of disrupting these structures (Berends et al., 2010; von Kockritz-Blickwede and Winstel, 2022). Intriguingly, Nuc-mediated degradation of NETs leads to the release of deoxyribonucleoside monophosphates that can be converted by the staphylococcal cell surface protein AdsA (adenosine synthase A) into death-effector deoxyribonucleosides (Thammavongsa et al., 2013; Tantawy et al., 2022). Notably, AdsA-derived death-effector deoxyribonucleosides such as deoxyadenosine (dAdo) and deoxyguanosine (dGuo) display toxigenic properties and contribute to immune cell death during acute and persistent *S. aureus* infections (Thammavongsa et al., 2013; Winstel et al., 2019; Tantawy et al., 2022). More precisely, dAdo and dGuo-triggered phagocyte cell death involves the uptake of dAdo and dGuo via human equilibrative nucleoside transporter 1 (hENT1), intracellular phosphorylation of dAdo and dGuo by adenosine kinase (ADK) and deoxycytidine kinase (dCK), and subsequent imbalanced expansion of intracellular dATP and dGTP pools which trigger caspase-3-dependent immune cell death (Winstel et al., 2018; Tantawy et al., 2022). Of note, genetic disruption of this metabolic cascade rendered macrophages resistant to AdsA-derived death-effector deoxyribonucleosides, leading to the accumulation of phagocytes within the deeper cavity of abscesses and accelerated clearance of staphylococci *in vivo* (Winstel et al., 2018; Winstel et al., 2019; Tantawy et al., 2022). Thus, elements of the mammalian purine salvage pathway represent attractive targets for the design of novel host-directed therapeutics that aim at boosting macrophage survival during acute and persistent *S. aureus* infections. In particular, pharmacological inhibition of dCK by small molecule inhibitors may terminate the intracellular conversion of *S. aureus*- and AdsA-derived death-effector deoxyribonucleosides into deoxyribonucleoside monophosphates and subsequent accumulation of apoptosis-triggering deoxyribonucleoside triphosphates in host phagocytes (Figure 1A). If so, *S. aureus*- and dAdo/dGuo-mediated macrophage cell death may efficiently be prevented thereby aiding in the clearance of staphylococci during abscess formation and persistent infections.

Here we provide proof of this concept by establishing a novel host-directed therapeutic strategy for therapy of staphylococcal infectious diseases. Specifically, we show that the dCK-specific small molecule inhibitor (*R*)-DI-87 (((*R*)-2-((1-(2-(4-methoxy-3-(2-morpholinoethoxy)phenyl)-5-methylthiazol-4-yl)ethyl)thio)pyrimidine-4,6-diamine), an orally active, well-tolerated clinical-stage anti-cancer drug (Figure 1B) (Poddar et al., 2020), protects host phagocytes from staphylococcal death-effector deoxyribonucleoside-

128 mediated cytotoxicity and caspase-3-dependent cell death. Our results further suggest that administration of
129 (*R*)-DI-87 boosts macrophage survival during abscess formation and thus improves clinical outcomes in *S.*
130 *aureus*-infected laboratory animals.
131
132 **Results**
133 **(*R*)-DI-87-mediated blockade of mammalian dCK protects host immune cells from staphylococcal death-**
134 **effector deoxyribonucleosides.** To analyze whether pharmacological inhibition of mammalian dCK may
135 represent a suitable strategy to protect host phagocytes from staphylococcal death-effector
136 deoxyribonucleosides, we initially took advantage of various tissue culture model systems and pre-incubated
137 human U937 monocytes (U937) or U937-derived macrophages (U937 MΦ) with (*R*)-DI-87. Controls received
138 vehicle only. Following pre-incubation, U937 or U937 MΦ were exposed to dAdo or dGuo and analyzed for
139 viability rates 48 hours post-intoxication. Of note, (*R*)-DI-87-mediated inhibition of mammalian dCK in U937
140 or U937 MΦ efficiently prevented dAdo- or dGuo-induced cell death in a dose-dependent manner (Figure 2A-
141 D; supplementary Figure 1A-D). Moreover, these effects resembled the phenotype of dCK-deficient U937 or
142 U937 MΦ, which were found to be refractory to dAdo- or dGuo-mediated cytotoxicity (Figure 2A-D) (Winstel
143 et al., 2018; Tantawy et al., 2022). In addition, we observed that pre-treatment of primary human $CD14^+$
144 monocytes or human monocyte-derived macrophages (HMDMs) with (*R*)-DI-87 blocked dAdo- or dGuo-
145 triggered cytotoxicity suggesting that dCK inhibition may suppress the toxigenic properties of staphylococcal
146 death-effector deoxyribonucleosides (Figure 2E-H). To test this conjecture, we expressed a soluble and
147 affinity-tagged recombinant form of *S. aureus* AdsA (hereafter termed rAdsA) in *Escherichia coli*, which was
148 purified, released of its affinity tag and subsequently used for cytotoxicity assays. Particularly, we incubated
149 rAdsA with either dAMP or dGMP according to a published protocol (Tantawy et al., 2022) and added the
150 resulting, dAdo- or dGuo-containing and filter-sterilized reaction products to U937 or U937 MΦ that received
151 (*R*)-DI-87 or were left untreated prior to intoxication. While enzymatic reactions that contained rAdsA and
152 purine deoxyribonucleoside monophosphates triggered cell death of human monocytes or macrophages in
153 this approach, (*R*)-DI-87-exposed cells were fully protected against the cytotoxic effect of dAdo and dGuo
154 further indicating that inhibition of mammalian dCK helps to neutralize *S. aureus* AdsA-derived death-effector
155 deoxyribonucleosides (Figure 2I-J). Collectively, these initial data demonstrate that (*R*)-DI-87 is a suitable small
156 molecule dCK inhibitor capable of preventing host immune cell death induced by toxigenic products of the
157 staphylococcal Nuc/AdsA pathway.
158
159 **(*R*)-DI-87 prevents death-effector deoxyribonucleoside-induced activation of apoptosis.** Earlier work
160 demonstrated that staphylococcal dAdo and dGuo target the mammalian purine salvage pathway to trigger

161 an exaggerated biogenesis of deoxyribonucleoside triphosphates, thereby igniting caspase-3-dependent host
162 immune cell death (Winstel et al., 2018; Winstel et al., 2019; Tantawy et al., 2022). Since the accumulation of
163 deoxyribonucleoside triphosphates and associated apoptotic signaling via cleavage of caspase-3 exclusively
164 occurs in dCK-proficient monocytes or macrophages upon intoxication with death-effector
165 deoxyribonucleosides such as dAdo (Winstel et al., 2018; Tantawy et al., 2022), it seemed plausible to us at
166 this stage that administration of (*R*)-DI-87 and inhibition of dCK may suppress dAdo- or dGuo-mediated
167 activation of the programmed cell death machinery. To test this hypothesis, U937 or U937 MΦ were pre-
168 incubated with (*R*)-DI-87, exposed to dAdo or dGuo, and used to generate cell extracts for evaluation of
169 caspase-3 activity by measuring the hydrolysis of the caspase-3-specific peptide substrate Ac-DEVD-pNA. As
170 expected, (*R*)-DI-87-treatment of U937 or U937 MΦ significantly decreased dAdo- or dGuo-mediated
171 activation of caspase-3 activity (Figure 3A-D). Since caspase-3 represents the key modulator of the apoptosis
172 signaling pathway, these data suggest that (*R*)-DI-87-mediated dCK inhibition selectively prevented dAdo- or
173 dGuo-mediated induction of apoptotic cell death in host immune cells (Figure 3A-D). To verify these results
174 further, cell extracts were also probed with a specific antibody capable of detecting the active (cleaved) form
175 of human caspase-3. In agreement with the enzymatic activity assay, (*R*)-DI-87-treatment of U937 or U937 MΦ
176 prevented caspase-3 activation (Figure 3E-F). Moreover, we exposed U937 phagocytes to (*R*)-DI-87 and
177 assessed dAdo- or dGuo-mediated activation of apoptotic signaling via immunofluorescence microscopy.
178 Microscopy-based analysis of (*R*)-DI-87- and death-effector deoxyribonucleoside-exposed macrophages
179 confirmed that (*R*)-DI-87 inhibited activation of programmed cell death and apoptosis as positive signals for
180 annexin-V/PI were strongly decreased in samples that have been exposed to the dCK inhibitor (Figure 3G-H).
181 Of note, similar findings were also obtained with primary HMDMs, suggesting that (*R*)-DI-87 is a suitable agent
182 to block death-effector deoxyribonucleoside-mediated induction of apoptosis in host phagocytes
183 (supplementary Figure 2). Together, these data indicate that administration of (*R*)-DI-87 and associated
184 inhibition of mammalian dCK prevents apoptotic cell death in phagocytes caused by *S. aureus* AdsA-derived
185 death-effector deoxyribonucleosides.
186
187 **Pharmacological inhibition of host dCK attenuates *S. aureus* virulence in a mouse model of bloodstream**
188 **infection.** To evaluate the therapeutic value and safety of (*R*)-DI-87 *in vivo*, cohorts of female C57BL/6 mice
189 received (*R*)-DI-87 (75 mg/kg) or vehicle (40% Captisol) via oral gavage in 12-hour intervals over a time period
190 of 16 days. On day 16, peripheral blood was collected from all cohorts of mice and subjected to a FACS-based
191 immuno-phenotyping approach (Figure 4A). Continuous treatment of animals with (*R*)-DI-87 did not alter the
192 immune cell composition of peripheral blood (Figure 4A). Further, animals treated with (*R*)-DI-87 did neither
193 lose weight nor displayed any other obvious phenotype during this procedure suggesting that (*R*)-DI-87

194 represents a safe and highly selective therapeutic agent (Figure 4B). Next, we sought to investigate whether
195 (*R*)-DI-87-mediated protection of mammalian phagocytes may represent a valuable strategy to cure
196 staphylococcal diseases and tested the therapeutic efficacy of the compound in a mouse model of *S. aureus*
197 bloodstream infection. In this model, C57BL/6 mice were treated with (*R*)-DI-87 (75 mg/kg) or vehicle (40%
198 Captisol) via oral gavage every 12 hours and challenged with a single dose of 1.0 x 10^7 CFU *S. aureus* Newman,
199 a human clinical isolate (Duthie and Lorenz, 1952). Five days post-infection, mice were euthanized. Livers and
200 kidneys were dissected and analyzed for visible abscess lesions. Subsequently, tissue homogenates were
201 prepared and plated on agar plates to measure bacterial loads in infected organs. Notably, abscess numbers
202 and bacterial loads were significantly reduced in livers and kidneys in (*R*)-DI-87-treated animals as compared
203 to control mice validating (*R*)-DI-87 as a novel host-directed and anti-infective drug against staphylococcal
204 diseases (Figure 4C-F). To test whether *S. aureus* exploits the activity of dCK along with the purine salvage
205 pathway during infection, cohorts of mice were also challenged with the *S. aureus* Newman *adsA* mutant. (*R*)-
206 DI-87-treated animals no longer displayed increased resistance to *S. aureus* infection (Figure 4C-F). Moreover,
207 infection with *S. aureus adsA*-deficient bacteria phenocopied (*R*)-DI-87-mediated inhibition of dCK, in line with
208 the concept that AdsA is required for establishing persistent infections in host tissues (Figure 4C-F). In light of
209 these findings, infected organs were also fixed with formalin, embedded into paraffin, thin-sectioned, and
210 analyzed for histopathology. As expected, histopathological analysis of hematoxylin and eosin (H&E)-stained
211 liver or renal tissues revealed that wild-type *S. aureus* Newman formed structured abscesses in vehicle-treated
212 mice (Figure 4G-H). However, lesions obtained from (*R*)-DI-87-treated animals appeared smaller in size and
213 typically did not harbor a discernable organization of staphylococci, further demonstrating that administration
214 of (*R*)-DI-87 represents a medically valuable strategy to attenuate staphylococcal virulence (Figure 4G-H).
215 Presumably, (*R*)-DI-87-treatment protects macrophages against AdsA-derived death-effector
216 deoxyribonucleosides and therefore enhances phagocyte survival during abscess formation as (*R*)-DI-87
217 neither improved the killing of *S. aureus* in human or mouse blood, nor it displayed antimicrobial activity
218 (supplementary Figure 3A-B; supplementary Table 1). Collectively, these data indicate that inhibition of
219 mammalian dCK by (*R*)-DI-87 attenuates *S. aureus* abscess formation and disease pathogenesis *in vivo*.
220
221 **(*R*)-DI-87-treatment amplifies macrophage infiltration into staphylococcal infectious foci.** Previous studies
222 revealed that macrophages with defects in the purine salvage pathway-apoptosis axis are refractory to
223 staphylococcal dAdo or dGuo (Winstel et al., 2018; Winstel et al., 2019; Tantawy et al., 2022). As a result,
224 death-effector deoxyribonucleoside-resistant tissue macrophages were found to accumulate within deep-
225 seated abscesses of *S. aureus*-challenged mice, a phenomenon that contributed to accelerated clearance of
226 staphylococci (Winstel et al., 2019). Thus, we hypothesized that pharmacological inhibition of host dCK might

227 augment phagocyte infiltration into *S. aureus*-derived abscesses, thereby explaining reduced bacterial burdens
228 in (*R*)-DI-87-treated laboratory animals. To pursue this possibility, we established an immunofluorescence
229 microscopy-based approach to detect macrophages in liver or renal tissues of *S. aureus* Newman wild type-
230 infected C57BL/6 mice that were treated with (*R*)-DI-87 or vehicle only. As expected, immunofluorescence
231 staining of tissue abscesses obtained from vehicle-treated animals revealed that F4/80-positive macrophages
232 resided at the periphery of infectious foci (Figure 5A-D). On the contrary, lesions derived from mice that
233 received (*R*)-DI-87 differed as they contained infiltrates of F4/80-positive macrophages within the neutrophil
234 cuff, suggesting that (*R*)-DI-87-mediated inhibition of host dCK terminates macrophage exclusion from
235 staphylococcal abscesses (Figure 5E-H). To further delineate whether these results correlate with AdsA and
236 staphylococcal death-effector deoxyribonucleoside-mediated manipulation of host dCK in phagocytes, tissues
237 of *S. aureus* Newman *adsA* mutant-infected mice, which received either (*R*)-DI-87 or vehicle, were also
238 examined via immunofluorescence microscopy and analyzed for the presence of F4/80-positive macrophages.
239 Of note, *adsA* mutant-derived abscess lesions were also characterized by increased infiltration rates of F4/80-
240 positive phagocytes, irrespectively of whether animals were treated with (*R*)-DI-87 or vehicle during the course
241 of the infection (Figure 5I-P). Thus, (*R*)-DI-87-mediated blockade of host dCK phenocopied the *adsA* mutation
242 in *S. aureus*. Lastly, (*R*)-DI-87- or vehicle-treated murine bone marrow-derived macrophages (BMDMs) mice
243 were analyzed for survival rates upon exposure to dAdo or dGuo. Compared to vehicle-treated cells, which
244 were susceptible to death-effector deoxyribonucleosides, BMDMs exposed to (*R*)-DI-87 displayed increased
245 resistance toward dAdo and dGuo presumably explaining their abundance in infectious foci obtained from
246 wild-type *S. aureus* Newman-challenged and dCK inhibitor-treated mice (Figure 5Q-R). In summary, these data
247 suggest that (*R*)-DI-87-treatment protects macrophages from staphylococcal death-effector
248 deoxyribonucleosides and therefore boosts their infiltration into persistent abscesses in organ tissues (Figure
249 6).
250

251 **Discussion**

252 Bacterial infectious diseases are typically treated with specific or broad-spectrum antibiotics. However, many
253 microbial pathogens have developed resistance mechanisms against these drugs and other antimicrobial
254 agents either via mutational changes within the drug target or by importing resistance genes from other
255 bacteria (Klevens et al., 2008; Yaw et al., 2014; Nubel, 2016; Jian et al., 2021; GBD 2019 Antimicrobial
256 Resistance Collaborators, 2022a). Accordingly, infections by multidrug-resistant microbes are frequently
257 associated with failure of therapy and increased mortality in both, industrialized and developing countries
258 around the world (Klevens et al., 2008; Yaw et al., 2014; GBD 2019 Antimicrobial Resistance Collaborators,

259 2022a; b). Each year, several million people die due to infections caused by drug-resistant bacteria such as
260 *Mycobacterium tuberculosis*, *E. coli*, or *S. aureus* underscoring the very urgent need of new therapeutics and
261 anti-infective compounds against which bacteria cannot develop resistance (Pai et al., 2016; GBD 2019
262 Antimicrobial Resistance Collaborators, 2022a; b).

263 Host-directed therapy is an emerging therapeutic concept that eliminates the possibility of drug
264 resistance development in microbial pathogens (Kaufmann et al., 2018). This innovative approach aims at
265 targeting specific host determinants and signaling cascades bacterial or other pathogenic microorganisms may
266 attack or exploit to establish acute and persistent infections (Kaufmann et al., 2018). Overall, this strategy
267 seeks to ameliorate host immunity, immune cell survival, and immunopathology, as well as pathogen control
268 without interfering with microbial replication, growth, or metabolism (Kaufmann et al., 2018). By applying this
269 concept along with a drug-repurposing approach, we here report that administration of (*R*)-DI-87, a soluble,
270 orally active, and high-affinity inhibitor of host dCK (Poddar et al., 2020), attenuates *S. aureus* virulence in a
271 mouse model of bloodstream infection. In particular, we show that (*R*)-DI-87-mediated blockade of host dCK
272 prevents staphylococcal death-effector deoxyribonucleoside-triggered apoptotic cell death in phagocytes of
273 human and animal origin. Accordingly, oral administration of (*R*)-DI-87 in mice rendered host phagocytes
274 refractory to AdsA-derived dAdo and dGuo thereby leading to an accumulation of *S. aureus*-eliminating
275 macrophages within deeper cavities of infectious foci along with accelerated phagocytic clearance of
276 staphylococci. Since dCK is a rate-limiting enzyme of the nucleoside salvage pathway that catalyzes the
277 intracellular conversion of deoxyribonucleosides into deoxyribonucleoside monophosphates (Arner and
278 Eriksson, 1995), (*R*)-DI-87-mediated inhibition of dCK most likely suppresses an uncontrolled biogenesis of
279 deoxyribonucleoside di- and triphosphates that may trigger replication errors and apoptosis in host cells.
280 Consistent with this model, earlier work suggested that dCK deficiency in phagocytes or other cells such as
281 lymphoblasts prevents an overload of intracellular deoxyribonucleoside triphosphates upon exposure to
282 death-effector deoxyribonucleosides (Gudas et al., 1978; Winstel et al., 2018). Thus, inhibition of host dCK
283 represents an attractive host-directed therapeutic intervention strategy that terminates a refined immune-
284 evasive maneuver *S. aureus* has evolved to establish persistent infections in mammalian hosts. The
285 technological advantage of this therapeutic approach, beyond the clinical importance and long-term economic
286 benefits for the medical-therapeutic sector, is undoubtedly the exploitation of an already existing, highly
287 selective, and clinical-stage compound that can easily be administered to attenuate infections caused by a
288 predominant bacterial pathogen. In particular, (*R*)-DI-87 does not exhibit detrimental side effects as (*R*)-DI-87-
289 exposed laboratory animals neither lost weight during long-term treatment nor displayed any other adverse
290 effects that may negatively affect host immune responses. Specifically, the immune cell composition profile
291 of mice that received (*R*)-DI-87 was not altered when compared to mice that received the vehicle control. This

292 suggests that patrolling neutrophils known to play a significant role during staphylococcal infections (Spaan et
293 al., 2013) along with other crucial elements of the host immune system are fully functional in (*R*)-DI-87-treated
294 hosts, thereby offering tremendous opportunities to improve infection outcomes in hospitalized or critically
295 ill patients. Further, usage of (*R*)-DI-87 represents a host-directed and anti-infective therapeutic approach to
296 which *S. aureus* and other multidrug-resistant bacteria cannot develop resistance mechanisms. In this regard,
297 we note that many other medically highly relevant bacterial pathogens including streptococci, *Bacillus*
298 *anthracis*, and multidrug-resistant *Staphylococcus pseudintermedius* synthesize effector-nucleosides in order
299 to modulate host immune cell responses (Thammavongsa et al., 2009; Liu et al., 2014; Zheng et al., 2015; Ma
300 et al., 2017; Dai et al., 2018; Bunsow et al., 2021). Thus, (*R*)-DI-87-mediated inhibition of dCK may also help to
301 protect host cells from apoptotic cell death or other adverse effects during other bacterial diseases in human
302 or animal hosts. Even polymicrobial infections caused by various microbial pathogens and other infectious
303 agents that manipulate the purine salvage pathway-apoptosis axis during infection can eventually be
304 prevented, attenuated, or cured by using (*R*)-DI-87. Ultimately, double-pronged therapies which cover the
305 usage of (*R*)-DI-87 combined with antibiotics, various anti-infective agents, or monoclonal antibodies, some of
306 which are known to neutralize predominant staphylococcal virulence determinants, including secreted toxins
307 (Ragle and Bubeck Wardenburg, 2009; Hua et al., 2014; Thomsen et al., 2017), protein A (Kim et al., 2012;
308 Chen et al., 2022b), and specific surface antigens (Bennett et al., 2019; de Vor et al., 2022) along with usage
309 of other host-directed therapeutics that impede *S. aureus* disease pathogenesis (Bravo-Santano et al., 2019;
310 Alphonse et al., 2021), may essentially improve disease progression during severe bacterial infectious diseases
311 and should therefore be considered for pre-clinical tests in animal models.

312 Overall, (*R*)-DI-87-mediated inhibition of dCK is a novel host-directed therapeutic concept to improve
313 clinical outcomes of *S. aureus* infectious diseases. Since (*R*)-DI-87 is extremely well tolerated in humans
314 (personal communication; Kenneth A. Schultz, Trethera Corporation, Los Angeles, CA, USA) and currently
315 being investigated in phase I clinical trials for the treatment of non-communicable diseases, including cancer
316 and multiple sclerosis (Poddar et al., 2020; Chen et al., 2022a), this compound already meets the requirements
317 for a prompt launch of clinical studies in individuals that suffer local or invasive staphylococcal infections.
318 Optimization of (*R*)-DI-87 or any medically acceptable derivatives thereof may further accelerate this process
319 and concurrently could also aid in the design of pre-exposure prophylactic agents for hospitalized or high-risk
320 patients, with the primary aim to enhance infection control and public health.

321

322 **Materials und methods**

323 **Bacterial strains and growth conditions.** All bacterial strains used in this study are listed in the *Supplementary*
324 *Materials* (supplementary Table 2). Bacteria were grown in tryptic soy broth (TSB), Mueller-Hinton broth

325 (MHB), or lysogeny broth (LB) at permissive temperatures. Media were supplemented with appropriate
326 antibiotics (ampicillin 100 µg/ml).

327 **Cell lines and tissue culture.** U937 cells were obtained from American Type Culture Collection (ATCC) and
328 grown in Roswell Park Memorial Institute (RPMI) 1640 medium (Gibco) supplemented with 10% heat-
329 inactivated fetal bovine serum (hi-FBS) according to the manufacturer's instructions. All mammalian cell lines
330 were grown at 37°C under 5% CO_2. Cell lines used in this study are listed in the *Supplementary Materials*
331 (supplementary Table 3).

332 **Isolation of human primary cells.** Peripheral blood mononuclear cells (PBMCs) were isolated from heparinized
333 blood by density gradient centrifugation on Pancoll (PAN Biotech) according to standard laboratory protocols.
334 Next, human primary monocytes were isolated from PBMCs by using magnetic nanobeads and the MojoSort™
335 Human CD14 Selection Kit (BioLegend) as described earlier (Tantawy et al., 2022). Subsequently, purified
336 primary CD14-positive ($CD14^+$) monocytes were resuspended in RPMI 1640 medium containing 10% hi-FBS
337 and 1% penicillin-streptomycin and used for cytotoxicity assays. Alternatively, purified $CD14^+$ monocytes were
338 differentiated into human monocyte-derived macrophages (HMDMs) in the same medium supplemented with
339 50 ng/ml of human macrophage colony stimulating factor (hM-CSF; Genscript). HMDMs were used at day 7
340 post-differentiation for cytotoxicity experiments.

341 **Isolation of murine bone marrow-derived macrophages.** Bone marrow-derived macrophages (BMDMs) were
342 isolated from C57BL/6 mice as previously described (Tantawy et al., 2022). In brief, mice were euthanized to
343 remove the femur and tibia which were sterilized by using 70% ethanol. Bones were then washed with sterile
344 phosphate-buffered saline (PBS). Next, the bone ends were removed and the bone marrow was flushed out
345 by using RPMI 1640 containing 10% hi-FBS and 1% penicillin-streptomycin. Following a resuspension step, cells
346 were passed through a nylon cell strainer (40 µm) to remove unwanted tissue and cellular debris.
347 Subsequently, cells were centrifuged (10 min, 200 x g, 4°C), resuspended in red blood cell (RBC) lysis buffer
348 (Roche), and incubated for 5 min at room temperature to lyse RBC. Cells were centrifuged once more,
349 resuspended in BMDM medium (RPMI 1640 containing 10% hi-FBS, 1% penicillin-streptomycin, and 50 ng/ml
350 of mouse macrophage colony-stimulating factor (Genscript)), and seeded into tissue culture-treated dishes to
351 deplete bone marrow cells from fibroblasts. At day 1 post-extraction, suspension bone marrow cells were
352 collected via centrifugation, adjusted to 6.0 x 10^5 cells/ml in BMDM medium, and re-seeded into
353 bacteriological dishes. At day 4 post-extraction, cells were incubated with an additional 10 ml of BMDM
354 medium. BMDMs were used at day 7 post-extraction for cytotoxicity experiments.

355 **Protein purification.** Purification of recombinant *S. aureus* AdsA was performed as described elsewhere
356 (Thammavongsa et al., 2009; Tantawy et al., 2022). Briefly, a glutathione S-transferase (GST)-tagged and
357 recombinant version of *S. aureus* AdsA (rAdsA) was expressed in *E. coli* BL21 using the pGEX-2T plasmid system
358 (GE Healthcare) and purified via glutathione S-transferase affinity chromatography (Thammavongsa et al.,
359 2009; Tantawy et al., 2022). Next, the N-terminal GST tag was removed by using thrombin which was
360 immediately cleared from the protein sample via benzamidine sepharose beads according to the
361 manufacturer's instructions (GE Healthcare). Purified rAdsA was analyzed by a Coomassie-stained SDS-PAGE
362 following standard laboratory protocols.

363 **Cytotoxicity assays.** To evaluate the protective role of (*R*)-DI-87 during death-effector deoxyribonucleoside-
364 induced cytotoxicity, 2.0 x 10^5 U937 monocyte-like cells (U937) per well were seeded in a 24-well plate and
365 pre-incubated for 2 h at 37°C under 5% CO_2 in RPMI 1640 medium containing 10% hi-FBS and 1 µM of (*R*)-DI-
366 87. Control wells received vehicle only. Alternatively, 4.0 × 10^5 U937 cells per well were seeded in a 24-well
367 plate and incubated for 48 h at 37°C under 5% CO_2 in RPMI 1640 growth medium that contained 160 nM
368 phorbol 12-myristate 13-acetate (PMA). Resulting U937-derived macrophages (U937 MΦ) were washed and
369 further incubated in RPMI 1640 growth medium lacking PMA (24 h). Similarly, 3.5 x 10^5 BMDMs per well were
370 seeded in 24-well plates and incubated for 24 h at 37°C under 5% CO_2 in corresponding growth media. Next,
371 U937 MΦ or BMDMs were washed once and pre-incubated for 2 h at 37°C under 5% CO_2 in appropriate growth
372 media supplemented with 1 µM of (*R*)-DI-87. Control wells received vehicle only. Following pre-incubation
373 with (*R*)-DI-87, U937, U937 MΦ, or BMDMs were exposed to various concentrations of either dAdo or dGuo
374 (100 µM for U937; 200 µM for U937 MΦ or BMDMs) and incubated for 48 h at 37°C under 5% CO_2 in RPMI
375 1640 growth medium. Cells were collected via centrifugation (U937) or a detachment-centrifugation step
376 using trypsin-EDTA (U937 MΦ) or accutase (BMDMs) solution. Dead cells were stained with trypan blue and
377 counted by using a microscope to calculate killing efficiency. To analyze the protective effect of (*R*)-DI-87 in
378 primary human cells, 2.0 x 10^5 $CD14^+$ monocytes or HMDMs per well were seeded in multi-well plates and pre-
379 incubated for 2 h at 37°C under 5% CO_2 in RPMI 1640 medium containing 10% hi-FBS and 1 µM of (*R*)-DI-87.
380 Control wells received vehicle only. Subsequently, cells were intoxicated by using various concentrations of
381 either dAdo or dGuo (100 µM for $CD14^+$ monocytes; 200 µM for HMDMs) and incubated in appropriate growth
382 media for 48 h at 37°C under 5% CO_2. Cells were collected via centrifugation ($CD14^+$ monocytes) or a
383 detachment-centrifugation step (HMDMs) using trypsin-EDTA solution. Viability of cells was determined via
384 trypan blue staining and microscopy as described above. To block the cytotoxic effect of AdsA-derived death-
385 effector deoxyribonucleosides by using (*R*)-DI-87, rAdsA (1.25 µg/µl) was incubated for 16 h at 37°C in a
386 reaction buffer (30 mM Tris-HCl, pH 7.5; 1.5 mM $MgCl_2$; 1.5 mM $MnCl_2$) supplemented with either dAMP or

387 dGMP (1.19 mM each) according to a published protocol (Tantawy et al., 2022). Controls included reactions
388 that lacked deoxyribonucleoside monophosphates or rAdsA. Following incubation, all reaction products were
389 filter-sterilized and added to U937 MΦ which were pre-incubated with vehicle or 1 µM (*R*)-DI-87 for 2 h prior
390 to intoxication. Next, cells were incubated at 37°C under 5% CO_2 for 48 h, collected, and analyzed via trypan
391 blue staining and microscopy as described above.

392 **Assessment of caspase-3-activity.** Caspase-3 activity was analyzed using a colorimetric caspase-3 detection
393 kit (Sigma) and a published protocol (Winstel et al., 2018; Tantawy et al., 2022). Briefly, U937 cells or U937
394 MΦ along with appropriate controls were pre-incubated for 2 h at 37°C under 5% CO_2 in RPMI 1640 medium
395 containing 10% hi-FBS and 1 µM of (*R*)-DI-87. Controls received vehicle only. Subsequently, cells were exposed
396 to various concentrations of either dAdo or dGuo (100 µM for U937; 200 µM for U937 MΦ) and incubated for
397 24 h at 37°C under 5% CO_2 in RPMI 1640 growth medium. Cells were collected via centrifugation (U937) or a
398 detachment-centrifugation step (U937 MΦ) using trypsin-EDTA solution and washed once in PBS. Next, 1.0 x
399 10^7 cells were lysed in pre-chilled lysis buffer (Sigma kit) for 20 min. This step was performed on ice. Resulting
400 lysates were centrifuged at 4°C (18,000 × g for 10 min) to obtain cell- and debris-free supernatants which were
401 incubated with the caspase-3 substrate Ac-DEVD-pNA according to the manufacturer's instructions. Caspase-
402 3 activity was determined based on the amount of released pNA that can be detected at 405 nm.

403 **Immunoblotting.** Immunoblotting was performed as described elsewhere (Tantawy et al., 2022). In short,
404 U937 or U937 MΦ and appropriate controls were pre-incubated for 2 h at 37°C under 5% CO_2 in RPMI 1640
405 medium containing 10% hi-FBS and 1 µM of (*R*)-DI-87. Controls received vehicle only. Next, cells were treated
406 with dAdo or dGuo (100 µM for U937; 200 µM for U937 MΦ), incubated for 24 h at 37°C under 5% CO_2 in RPMI
407 1640 growth medium, and collected via centrifugation (U937) or a detachment-centrifugation step (U937 MΦ)
408 using trypsin-EDTA solution. Cells were washed once in PBS. 1.0 x 10^7 cells were lysed on ice in pre-chilled lysis
409 buffer (50 mM HEPES, pH 7.4; 5 mM CHAPS; 5 mM DTT) for 20 min. Resulting lysates were centrifuged at 4°C
410 (18,000 × g for 10 min) to obtain cell- and debris-free supernatants which were mixed with sodium dodecyl
411 sulfate-polyacrylamide gel (SDS-PAGE) loading buffer. Samples were boiled for 10 min at 95°C. Proteins were
412 separated via SDS-PAGE (12%) and transferred onto PVDF membranes for immunoblot analysis with the
413 following rabbit primary antibodies: α-Caspase-3 (α-CASP3, 9662, Cell Signaling) and α-GAPDH (ab181602,
414 Abcam, loading control). Immunoreactive signals were revealed with a secondary antibody conjugated to
415 horseradish peroxidase (α-rabbit IgG, 7074, Cell Signaling). Horseradish peroxidase activity was detected with
416 enhanced chemiluminescent (ECL) substrate (Thermo Fisher).

417 **FITC-annexin-V/PI staining.** FITC-annexin-V/PI staining of U937 MΦ or HMDMs exposed to 1 µM (*R*)-DI-87 and
418 death-effector deoxyribonucleosides (200 µM dAdo or dGuo; 24 h at 37°C) along with appropriate controls
419 was performed by using FITC-annexin-V Apoptosis Detection Kit I (BD Biosciences) according to the
420 manufacturer's instructions. Stained cells were analyzed via immunofluorescence microscopy according to
421 standard laboratory protocols.

422 **Determination of the minimal inhibitory concentration (MIC).** The MIC of (*R*)-DI-87 was determined in 96-
423 well plates by using the microdilution method and Mueller-Hinton broth according to standard laboratory
424 protocols. Wells containing varying concentrations of (*R*)-DI-87 or vehicle were inoculated with 10^5 CFU/ml of
425 wild-type *S. aureus* Newman or its *adsA* mutant and incubated for 24 h at 37°C under continuous shaking. The
426 MIC was defined as the lowest concentration of compound at which no visible growth was detected.

427 **Bacterial survival in blood.** Bacterial survival in mouse or human blood was analyzed as described before
428 (Thammavongsa et al., 2009). In brief, fresh overnight cultures of *S. aureus* Newman wildtype or its *adsA* were
429 diluted into fresh TSB medium and grown at 37°C to an OD of 1.0. Bacteria were washed twice in sterile PBS
430 and adjusted in PBS to a final density of 1.0 x 10^8 CFU/ml. Next, freshly drawn mouse or human blood
431 anticoagulated with heparin was incubated in the presence or absence of 1 µM (*R*)-DI-87 for 60 min (37°C)
432 with *S. aureus* Newman wildtype or its *adsA* mutant using a bacterial dose of 1.0 x 10^6 CFU/ml (murine blood)
433 or 1.0 x 10^7 CFU/ml (human blood). Samples without (*R*)-DI-87 treatment received the vehicle. Following
434 incubation, blood samples were mixed in a 1:1 ratio with sterile lysis buffer (PBS containing 1.0% saponin) and
435 incubated for 10 min at 37°C to lyse eukaryotic cells. Subsequently, serial dilutions were prepared and plated
436 onto TSA plates to determine bacterial survival rates.

437 **Animal infection model.** C57BL/6 mice were purchased from Janvier Laboratories and kept under specific
438 pathogen-free conditions in our central mouse facility (TWINCORE, Center for Experimental and Clinical
439 Infection Research, Hannover, Germany). Mice received (*R*)-DI-87 (75 mg/kg) or vehicle (40% Captisol) via oral
440 gavage at the day of the infection, separated by 12-hour intervals over a 5-day observation period. For
441 infection experiments, TSB overnight cultures of wild-type *S. aureus* Newman or its *adsA* mutant were diluted
442 1:100 in TSB and grown to an optical density (600 nm) of 0.5. Bacteria were then centrifuged (10 min, RT,
443 8,000 × g), washed twice in sterile PBS, and adjusted to 10^8 CFU/ml. One hundred microliters of the bacterial
444 suspension (10^7 CFU) were administered intravenously (lateral tail vein) into 6- to 8-weeks-old female C57BL/6
445 mice. Five days post-infection, animals were euthanized. Organs were dissected, examined for surface
446 abscesses, and homogenized in sterile PBS supplemented with 0.1% Triton X-100. Serial dilutions were
447 prepared and plated onto TSA plates to determine bacterial loads. For histopathology, dissected organs were

448 fixed in 10% Formalin (Sigma), embedded into paraffin, thin-sectioned, and stained with hematoxylin and
449 eosin (H&E). Stained tissues were examined by microscopy according to standard laboratory protocols.

450 **Immunofluorescence staining.** To detect macrophages in *S. aureus*-infected tissues, formalin-fixed and
451 paraffin-embedded organs were thin-sectioned, deparaffinized, and rehydrated. After heat-induced antigen
452 retrieval in 10 mM sodium citrate buffer (pH 6.0), non-specific antibody binding was blocked by adding 2%
453 normal goat serum. Immunofluorescence staining was carried out by using an antibody against F4/80-positive
454 macrophages (α-F4/80, 70076, Cell Signaling), followed by a fluorescently-labelled secondary antibody
455 (Alexa546, Invitrogen). Stained tissues were examined by using a Zeiss Apotome 2 microscope (Zeiss).

456 **Safety assessment of (*R*)-DI-87.** To assess the therapeutic value and safety of (*R*)-DI-87, cohorts of female
457 C57BL/6 mice were treated with (*R*)-DI-87 (75 mg/kg) or vehicle (40% Captisol) via oral gavage in 12-hour
458 intervals over the course of 16 days. On day 16, 100 µl peripheral blood was collected in lithium heparin-
459 coated tubes via retro-orbital bleeding using heparin-coated capillary tubes. Subsequently, blood samples
460 were incubated with 5 ml of ACK lysis buffer at room temperature for 5 min, quenched with 5 ml of FACS
461 buffer (5% FBS in PBS), and centrifuged at 4°C (4 min). This process was repeated and cells were subsequently
462 stained with the following fluorochrome-conjugated anti-mouse antibodies diluted 1:100 in 100 µl of FACS
463 buffer for 20 min at 4°C: α-B220-PerCP/Cy5.5 (103236, BioLegend), α-CD4-BV711 (100550, BioLegend), α-
464 CD8α-PE (100708, BioLegend), α-CD11c-PE/Dazzle594 (117347, BioLegend), α-CD11b-FITC (101206,
465 BioLegend), α-GR1-APC (108412, BioLegend); α-CD16/32 (FC block; 101319; BioLegend). Following incubation,
466 cells were centrifuged and washed twice using FACS buffer. Cells were resuspended in FACS buffer and
467 analyzed using a BD LSRII flow cytometer and the FlowJo software package. During the (*R*)-DI-87 or vehicle
468 treatment procedure, mice were regularly monitored and weighed to assess the overall health status.

469 **Ethics statement.** All animal experiments were conducted in accordance with the local animal welfare
470 regulations reviewed by the institutional review board and the Niedersächsisches Landesamt für
471 Verbraucherschutz und Lebensmittelsicherheit (LAVES) under the permission number 33.19-42502-04-
472 21/3696. Scientific use of animals (murine blood samples; isolation of BMDMs) was further carried out under
473 approved animal care and use protocols which are granted by the state veterinary authorities and overseen
474 by the internal animal care and use committee (IACUC). Animal studies required to assess the safety of (*R*)-DI-
475 87 in mice were approved by the UCLA Animal Research Committee (ARC). Human blood samples were
476 obtained from adult, consenting healthy donors. Informed consent forms were obtained from all participants.
477 These studies were reviewed and approved by the medical ethics committee of Hannover Medical School
478 (Hannover, Germany) under the permission number 8831_BO_K_2019.

Synthesis and preparation of (*R*)-DI-87. (*R*)-DI-87 ((((*R*)-2-((1-(2-(4-methoxy-3-(2-morpholinoethoxy)phenyl)-5-methylthiazol-4-yl)ethyl)thio)pyrimidine-4,6-diamine) was synthesized as described before (Poddar et al., 2020). For experiments, (*R*)-DI-87 was either dissolved in Dimethyl sulfoxide (*in vitro* experiments) or in an aqueous solution containing 40% Captisol (CyDex Pharmaceuticals, Inc.) (*in vivo* experiments).

Statistical analysis. Statistical analysis was performed by using GraphPad Prism (GraphPad Software, Inc., La Jolla, USA). Statistically significant differences were calculated by using statistical methods as indicated. *P* values < 0.05 were considered significant.

Data availability. All data supporting the findings of this study are available within the article and its supplementary material. All other data are available from the corresponding author upon reasonable request.

Acknowledgments

We thank all laboratory members for helpful discussion. We are grateful for support from the German Research Foundation (award WI4582/2-1 to V.W., project number 449712894). E.R.A. is supported by UCLA Tumor Immunology Training Grant T32CA009120. This work was supported by National Institutes of Health grants to C.G.R. (1R01CA25052901A1 and 1R01CA260678-01).

Author contributions

Volker Winstel: Conceptualization; data curation; investigation; methodology; formal analysis; supervision; funding acquisition; writing – original draft; writing – review and editing; visualization; project administration. Evan R. Abt: Conceptualization; data curation; investigation; methodology; formal analysis; writing – review and editing. Caius G. Radu: Conceptualization; investigation; methodology; formal analysis; resources; funding acquisition; writing – review and editing.

Conflict of interest

C.G.R. is a co-inventor of the dCK inhibitor used in this study. This intellectual property has been patented by the University of California and optioned to Trethera Corporation, a company that C.G.R. owns equity in. V.W., E.R.A., and C.G.R. are inventors in a patent application covering the use of dCK inhibitors as a treatment for bacterial infectious diseases.

511 **References**

512 Alphonse MP, Rubens JH, Ortines RV, Orlando NA, Patel AM, Dikeman D, Wang Y, Vuong I, Joyce DP, Zhang J,
513 Mumtaz M, Liu H, Liu Q, Youn C, Patrick GJ, Ravipati A, Miller RJ, Archer NK, and Miller LS (2021). Pan-
514 caspase inhibition as a potential host-directed immunotherapy against MRSA and other bacterial skin
515 infections. *Sci Transl Med* 13(601). doi: 10.1126/scitranslmed.abe9887.
516 Arner ES, and Eriksson S (1995). Mammalian deoxyribonucleoside kinases. *Pharmacol Ther* 67(2)**,** 155-186. doi:
517 10.1016/0163-7258(95)00015-9.
518 Bennett MR, Bombardi RG, Kose N, Parrish EH, Nagel MB, Petit RA, Read TD, Schey KL, Thomsen IP, Skaar EP,
519 and Crowe JE (2019). Human mAbs to Staphylococcus aureus IsdA Provide Protection Through Both
520 Heme-Blocking and Fc-Mediated Mechanisms. *J Infect Dis* 219(8)**,** 1264-1273. doi:
521 10.1093/infdis/jiy635.
522 Berends ET, Horswill AR, Haste NM, Monestier M, Nizet V, and von Kockritz-Blickwede M (2010). Nuclease
523 expression by Staphylococcus aureus facilitates escape from neutrophil extracellular traps. *J Innate*
524 *Immun* 2(6)**,** 576-586. doi: 10.1159/000319909.
525 Bravo-Santano N, Stolting H, Cooper F, Bileckaja N, Majstorovic A, Ihle N, Mateos LM, Calle Y, Behrends V, and
526 Letek M (2019). Host-directed kinase inhibitors act as novel therapies against intracellular
527 Staphylococcus aureus. *Sci Rep* 9(1)**,** 4876. doi: 10.1038/s41598-019-41260-8.
528 Brinkmann V, Reichard U, Goosmann C, Fauler B, Uhlemann Y, Weiss DS, Weinrauch Y, and Zychlinsky A (2004).
529 Neutrophil extracellular traps kill bacteria. *Science* 303(5663)**,** 1532-1535. doi:
530 10.1126/science.1092385.
531 Bunsow D, Tantawy E, Ostermeier T, Bahre H, Garbe A, Larsen J, and Winstel V (2021). Methicillin-resistant
532 Staphylococcus pseudintermedius synthesizes deoxyadenosine to cause persistent infection.
533 *Virulence* 12(1)**,** 989-1002. doi: 10.1080/21505594.2021.1903691.
534 Chambers HF, and Deleo FR (2009). Waves of resistance: Staphylococcus aureus in the antibiotic era. *Nat Rev*
535 *Microbiol* 7(9)**,** 629-641. doi: 10.1038/nrmicro2200.
536 Chen BY, Salas JR, Trias AO, Perez Rodriguez A, Tsang JE, Guemes M, Le TM, Galic Z, Shepard HM, Steinman L,
537 Nathanson DA, Czernin J, Witte ON, Radu CG, Schultz KA, and Clark PM (2022a). Targeting
538 deoxycytidine kinase improves symptoms in mouse models of multiple sclerosis. *Immunology*. doi:
539 10.1111/imm.13569.
540 Chen X, Schneewind O, and Missiakas D (2022b). Engineered human antibodies for the opsonization and killing
541 of Staphylococcus aureus. *Proc Natl Acad Sci U S A* 119(4). doi: 10.1073/pnas.2114478119.
542 Cheng AG, DeDent AC, Schneewind O, and Missiakas D (2011). A play in four acts: Staphylococcus aureus
543 abscess formation. *Trends Microbiol* 19(5)**,** 225-232. doi: 10.1016/j.tim.2011.01.007.
544 Dai J, Lai L, Tang H, Wang W, Wang S, Lu C, Yao H, Fan H, and Wu Z (2018). Streptococcus suis synthesizes
545 deoxyadenosine and adenosine by 5'-nucleotidase to dampen host immune responses. *Virulence* 9(1)**,**
546 1509-1520. doi: 10.1080/21505594.2018.1520544.
547 de Vor L, van Dijk B, van Kessel K, Kavanaugh JS, de Haas C, Aerts PC, Viveen MC, Boel EC, Fluit AC, Kwiecinski
548 JM, Krijger GC, Ramakers RM, Beekman FJ, Dadachova E, Lam MG, Vogely HC, van der Wal BC, van
549 Strijp JA, Horswill AR, Weinans H, et al. (2022). Human monoclonal antibodies against Staphylococcus
550 aureus surface antigens recognize in vitro and in vivo biofilm. *Elife* 11. doi: 10.7554/eLife.67301.
551 Duthie ES, and Lorenz LL (1952). Staphylococcal coagulase; mode of action and antigenicity. *J Gen Microbiol*
552 6(1-2)**,** 95-107. doi: 10.1099/00221287-6-1-2-95.
553 Finlay BB, and McFadden G (2006). Anti-immunology: evasion of the host immune system by bacterial and
554 viral pathogens. *Cell* 124(4)**,** 767-782. doi: 10.1016/j.cell.2006.01.034.
555 Foster TJ (2005). Immune evasion by staphylococci. *Nat Rev Microbiol* 3(12)**,** 948-958. doi:
556 10.1038/nrmicro1289.

557 Fridkin SK, Hageman JC, Morrison M, Sanza LT, Como-Sabetti K, Jernigan JA, Harriman K, Harrison LH, Lynfield
558 R, and Farley MM (2005). Methicillin-resistant *Staphylococcus aureus* disease in three communities.
559 *N. Engl. J. Med.* 352**,** 1436-1444.
560 GBD 2019 Antimicrobial Resistance Collaborators (2022a). Global burden of bacterial antimicrobial resistance
561 in 2019: a systematic analysis. *Lancet* 399(10325)**,** 629-655. doi: 10.1016/S0140-6736(21)02724-0.
562 GBD 2019 Antimicrobial Resistance Collaborators (2022b). Global mortality associated with 33 bacterial
563 pathogens in 2019: a systematic analysis for the Global Burden of Disease Study 2019. *Lancet*
564 400(10369)**,** 2221-2248. doi: 10.1016/S0140-6736(22)02185-7.
565 Gudas LJ, Ullman B, Cohen A, and Martin DW, Jr. (1978). Deoxyguanosine toxicity in a mouse T lymphoma:
566 relationship to purine nucleoside phosphorylase-associated immune dysfunction. *Cell* 14(3)**,** 531-538.
567 doi: 10.1016/0092-8674(78)90239-8.
568 Hua L, Hilliard JJ, Shi Y, Tkaczyk C, Cheng LI, Yu X, Datta V, Ren S, Feng H, Zinsou R, Keller A, O'Day T, Du Q,
569 Cheng L, Damschroder M, Robbie G, Suzich J, Stover CK, and Sellman BR (2014). Assessment of an anti-
570 alpha-toxin monoclonal antibody for prevention and treatment of Staphylococcus aureus-induced
571 pneumonia. *Antimicrob Agents Chemother* 58(2)**,** 1108-1117. doi: 10.1128/AAC.02190-13.
572 Jian Z, Zeng L, Xu T, Sun S, Yan S, Yang L, Huang Y, Jia J, and Dou T (2021). Antibiotic resistance genes in bacteria:
573 Occurrence, spread, and control. *J Basic Microbiol* 61(12)**,** 1049-1070. doi: 10.1002/jobm.202100201.
574 Kaufmann SHE, Dorhoi A, Hotchkiss RS, and Bartenschlager R (2018). Host-directed therapies for bacterial and
575 viral infections. *Nat Rev Drug Discov* 17(1)**,** 35-56. doi: 10.1038/nrd.2017.162.
576 Kim HK, Emolo C, DeDent AC, Falugi F, Missiakas DM, and Schneewind O (2012). Protein A-specific monoclonal
577 antibodies and prevention of Staphylococcus aureus disease in mice. *Infect Immun* 80(10)**,** 3460-3470.
578 doi: 10.1128/IAI.00230-12.
579 Klevens RM, Edwards JR, Gaynes RP, and National Nosocomial Infections Surveillance S (2008). The impact of
580 antimicrobial-resistant, health care-associated infections on mortality in the United States. *Clin Infect*
581 *Dis* 47(7)**,** 927-930. doi: 10.1086/591698.
582 Klevens RM, Morrison MA, Nadle J, Petit S, Gershman K, Ray S, Harrison LH, Lynfield R, Dumyati G, Townes JM,
583 Craig AS, Zell ER, Fosheim GE, McDougal LK, Carey RB, and Fridkin SK (2007). Invasive methicillin-
584 resistant *Staphylococcus aureus* infections in the United States. *JAMA* 298**,** 1763-1771.
585 Kuehnert MJ, Kruszon-Moran D, Hill HA, McQuillan G, McAllister SK, Fosheim G, McDougal LK, Chaitram J,
586 Jensen B, Fridkin SK, Killgore G, and Tenover FC (2006). Prevalence of *Staphylococcus aureus* nasal
587 colonization in the United States, 2001-2002. *J. Infect. Dis.* 193**,** 172-179.
588 Lee AS, de Lencastre H, Garau J, Kluytmans J, Malhotra-Kumar S, Peschel A, and Harbarth S (2018). Methicillin-
589 resistant Staphylococcus aureus. *Nat Rev Dis Primers* 4**,** 18033. doi: 10.1038/nrdp.2018.33.
590 Liu P, Pian Y, Li X, Liu R, Xie W, Zhang C, Zheng Y, Jiang Y, and Yuan Y (2014). Streptococcus suis adenosine
591 synthase functions as an effector in evasion of PMN-mediated innate immunit. *J Infect Dis* 210(1)**,** 35-
592 45. doi: 10.1093/infdis/jiu050.
593 Lowy FD (1998). Staphylococcus aureus infections. *N Engl J Med* 339(8)**,** 520-532. doi:
594 10.1056/NEJM199808203390806.
595 Ma F, Guo X, and Fan H (2017). Extracellular Nucleases of Streptococcus equi subsp. zooepidemicus Degrade
596 Neutrophil Extracellular Traps and Impair Macrophage Activity of the Host. *Appl Environ Microbiol*
597 83(2). doi: 10.1128/AEM.02468-16.
598 McKenna M (2013). Antibiotic resistance: the last resort. *Nature* 499(7459)**,** 394-396. doi: 10.1038/499394a.
599 Meka VG, and Gold HS (2004). Antimicrobial resistance to linezolid. *Clin Infect Dis* 39(7)**,** 1010-1015. doi:
600 10.1086/423841.
601 Nubel U (2016). Emergence and Spread of Antimicrobial Resistance: Recent Insights from Bacterial Population
602 Genomics. *Curr Top Microbiol Immunol* 398**,** 35-53. doi: 10.1007/82_2016_505.
603 Okumura CY, and Nizet V (2014). Subterfuge and sabotage: evasion of host innate defenses by invasive gram-
604 positive bacterial pathogens. *Annu Rev Microbiol* 68**,** 439-458. doi: 10.1146/annurev-micro-092412-
605 155711.

606 Pai M, Behr MA, Dowdy D, Dheda K, Divangahi M, Boehme CC, Ginsberg A, Swaminathan S, Spigelman M,
607 Getahun H, Menzies D, and Raviglione M (2016). Tuberculosis. *Nat Rev Dis Primers* 2**,** 16076. doi:
608 10.1038/nrdp.2016.76.
609 Poddar S, Capparelli EV, Rosser EW, Gipson RM, Wei L, Le T, Jung ME, Radu C, and Nikanjam M (2020).
610 Development and preclinical pharmacology of a novel dCK inhibitor, DI-87. *Biochem Pharmacol* 172**,**
611 113742. doi: 10.1016/j.bcp.2019.113742.
612 Ragle BE, and Bubeck Wardenburg J (2009). Anti-alpha-hemolysin monoclonal antibodies mediate protection
613 against Staphylococcus aureus pneumonia. *Infect Immun* 77(7)**,** 2712-2718. doi: 10.1128/IAI.00115-
614 09.
615 Spaan AN, Surewaard BG, Nijland R, and van Strijp JA (2013). Neutrophils versus Staphylococcus aureus: a
616 biological tug of war. *Annu Rev Microbiol* 67**,** 629-650. doi: 10.1146/annurev-micro-092412-155746.
617 Tantawy E, Schwermann N, Ostermeier T, Garbe A, Bahre H, Vital M, and Winstel V (2022). Staphylococcus
618 aureus Multiplexes Death-Effector Deoxyribonucleosides to Neutralize Phagocytes. *Front Immunol* 13**,**
619 847171. doi: 10.3389/fimmu.2022.847171.
620 Thammavongsa V, Kern JW, Missiakas DM, and Schneewind O (2009). Staphylococcus aureus synthesizes
621 adenosine to escape host immune responses. *J Exp Med* 206(11)**,** 2417-2427. doi:
622 10.1084/jem.20090097.
623 Thammavongsa V, Kim HK, Missiakas D, and Schneewind O (2015). Staphylococcal manipulation of host
624 immune responses. *Nat Rev Microbiol* 13(9)**,** 529-543. doi: 10.1038/nrmicro3521.
625 Thammavongsa V, Missiakas DM, and Schneewind O (2013). Staphylococcus aureus degrades neutrophil
626 extracellular traps to promote immune cell death. *Science* 342(6160)**,** 863-866. doi:
627 10.1126/science.1242255.
628 Thomsen IP, Sapparapu G, James DBA, Cassat JE, Nagarsheth M, Kose N, Putnam N, Boguslawski KM, Jones LS,
629 Wood JB, Creech CB, Torres VJ, and Crowe JE, Jr. (2017). Monoclonal Antibodies Against the
630 Staphylococcus aureus Bicomponent Leukotoxin AB Isolated Following Invasive Human Infection
631 Reveal Diverse Binding and Modes of Action. *J Infect Dis* 215(7)**,** 1124-1131. doi: 10.1093/infdis/jix071.
632 Tong SY, Davis JS, Eichenberger E, Holland TL, and Fowler VG, Jr. (2015). Staphylococcus aureus infections:
633 epidemiology, pathophysiology, clinical manifestations, and management. *Clin Microbiol Rev* 28(3)**,**
634 603-661. doi: 10.1128/CMR.00134-14.
635 Torres A, Cilloniz C, Niederman MS, Menendez R, Chalmers JD, Wunderink RG, and van der Poll T (2021).
636 Pneumonia. *Nat Rev Dis Primers* 7(1)**,** 25. doi: 10.1038/s41572-021-00259-0.
637 von Kockritz-Blickwede M, and Winstel V (2022). Molecular Prerequisites for Neutrophil Extracellular Trap
638 Formation and Evasion Mechanisms of Staphylococcus aureus. *Front Immunol* 13**,** 836278. doi:
639 10.3389/fimmu.2022.836278.
640 Wenzel RP (2007). Health care-associated infections: major issues in the early years of the 21st century. *Clin*
641 *Infect Dis* 45 Suppl 1**,** S85-88. doi: 10.1086/518136.
642 Winstel V, Missiakas D, and Schneewind O (2018). Staphylococcus aureus targets the purine salvage pathway
643 to kill phagocytes. *Proc Natl Acad Sci U S A* 115(26)**,** 6846-6851. doi: 10.1073/pnas.1805622115.
644 Winstel V, Schneewind O, and Missiakas D (2019). Staphylococcus aureus Exploits the Host Apoptotic Pathway
645 To Persist during Infection. *mBio* 10(6)**,** e02270-02219. doi: 10.1128/mBio.02270-19.
646 Yaw LK, Robinson JO, and Ho KM (2014). A comparison of long-term outcomes after meticillin-resistant and
647 meticillin-sensitive Staphylococcus aureus bacteraemia: an observational cohort study. *Lancet Infect*
648 *Dis* 14(10)**,** 967-975. doi: 10.1016/S1473-3099(14)70876-X.
649 Zheng L, Khemlani A, Lorenz N, Loh JM, Langley RJ, and Proft T (2015). Streptococcal 5'-Nucleotidase A (S5nA),
650 a Novel Streptococcus pyogenes Virulence Factor That Facilitates Immune Evasion. *J Biol Chem*
651 290(52)**,** 31126-31137. doi: 10.1074/jbc.M115.677443.

652

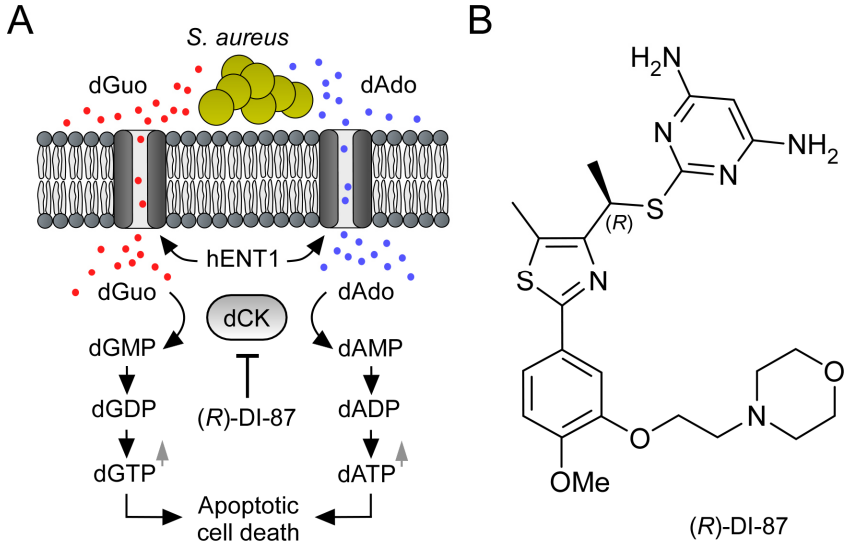

Figure 1. Mode of action of the dCK-specific inhibitor (*R*)-DI-87. (A) Scheme illustrating the mode of action of the dCK-specific inhibitor (*R*)-DI-87. *S. aureus*-derived dAdo and dGuo are pumped into phagocytes via human equilibrative transporter 1 (hENT1). Deoxycytidine kinase (dCK) converts dAdo and dGuo into appropriate deoxyribonucleoside monophosphates thereby triggering an accumulation of apoptosis-stimulating deoxyribonucleoside di- and triphosphates. (*R*)-DI-87 interferes with this pathway by inhibiting dCK, thus preventing host cell death. **(B)** Structure of (*R*)-DI-87.

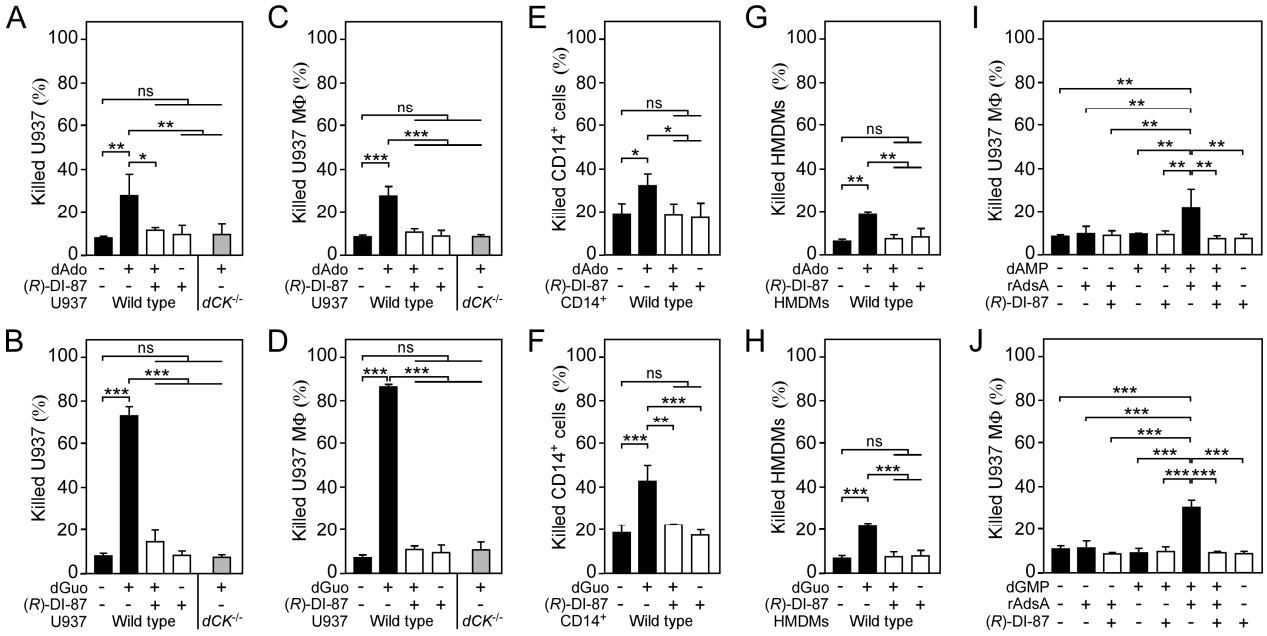

Figure 2. (*R*)-DI-87 protects phagocytes from death-effector deoxyribonucleoside-mediated cytotoxicity. (A-D) Survival rates of human U937 monocyte-like cells (U937) (A, B) or U937-derived macrophages (U937 MΦ) (C, D) exposed to dAdo or dGuo in the presence (+) or absence (-) of 1 µM (*R*)-DI-87. Cells were also exposed to the inhibitor or vehicle only. U937 *dCK*$^{-/-}$ were included as a control. **(E-H)** Survival rates of human CD14^{+} monocytes (E, F) or human monocyte-derived macrophages (HMDMs) (G, H) exposed to dAdo or dGuo in the presence (+) or absence (-) of 1 µM (*R*)-DI-87. Cells were also exposed to the inhibitor or vehicle only. **(I-J)** Survival rates of U937 MΦ exposed to rAdsA-derived dAdo (I) or dGuo (J). rAdsA was incubated with dAMP or dGMP and reaction products containing dAdo or dGuo were used to treat phagocytes in the presence (+) or absence (-) of 1 µM (*R*)-DI-87. Controls lacked rAdsA or deoxyribonucleoside monophosphates, or included reaction buffer only as indicated with + and − symbols. 100 µM (A-B; E-F) or 200 µM (C-D; G-H) of dAdo or dGuo were used to treat the cells. Cell survival rates were analyzed 48 h post-treatment. Data are the mean (± standard deviation [SD]) values from at least three independent determinations. Primary cell experiments include at least three independent donors. Statistically significant differences were analyzed with one-way analysis of variance (ANOVA) and Tukey's multiple-comparison test; ns, not significant ($P \geq 0.05$); *, $P < 0.05$; **, $P < 0.01$; ***, $P < 0.001$.

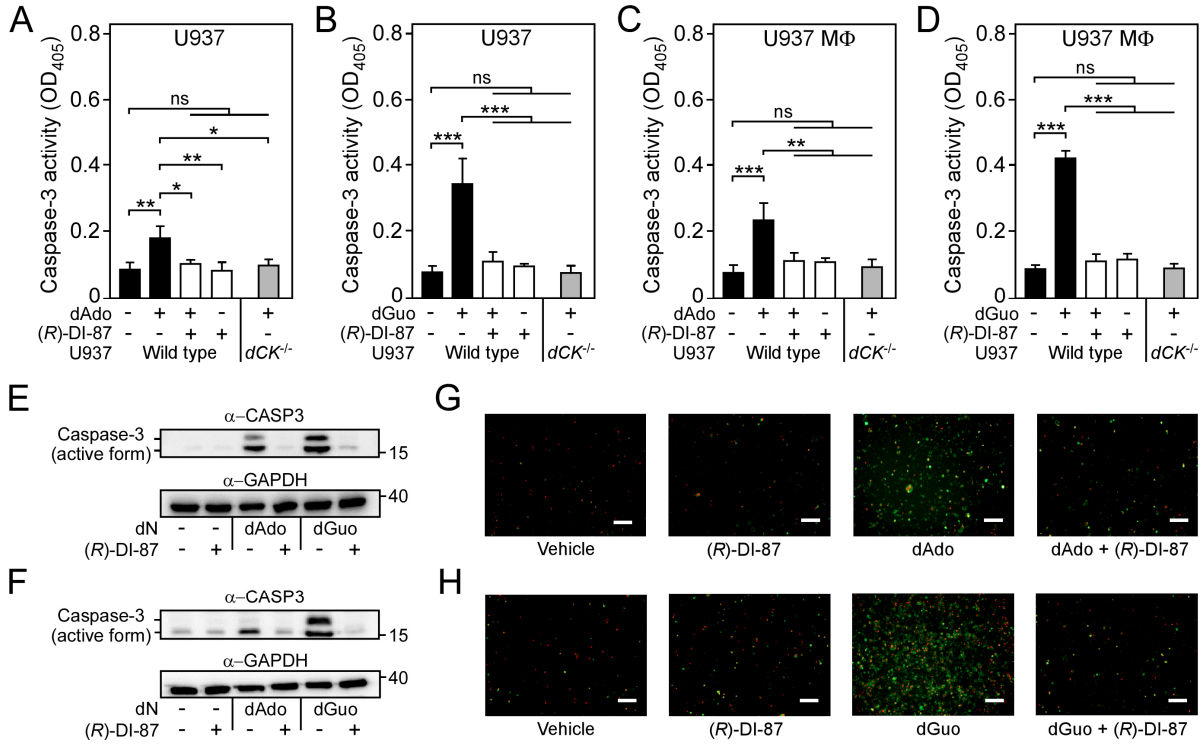

Figure 3. Selective inhibition of dCK prevents death-effector deoxyribonucleoside-mediated induction of immune cell apoptosis. (A-D) Analysis of caspase-3 activity in human U937 monocyte-like cells (U937) (A, B) or U937-derived macrophages (U937 MΦ) (C, D) exposed to dAdo or dGuo in the presence (+) or absence (-) of 1 µM (*R*)-DI-87. Cells were also exposed to the inhibitor or vehicle only. U937 *dCK*$^{-/-}$ were included as a control. Caspase-3 activity was analyzed using a colorimetric assay. **(E-F)** Immunoblotting of lysates obtained from U937 (E) or U937 MΦ (F) exposed to dAdo or dGuo in the presence (+) or absence (-) of 1 µM (*R*)-DI-87. Controls are indicated (+/– symbols). A specific antibody was used that detects the cleaved (active) form of caspase-3 (α-CASP3). GAPDH was used as a loading control (α-GAPDH). Numbers to the right of blots indicate the migration of molecular weight markers in kilodaltons. **(G-H)** Analysis of (*R*)-DI-87-dependent prevention of host cell apoptosis via immunofluorescence microscopy. U937 MΦ were exposed to dAdo (G) or dGuo (H) in the presence or absence of 1 µM (*R*)-DI-87 and stained using FITC-annexin-V/PI. Controls are indicated. White bars depict a length of 100 µm. Representative images are shown. 100 µM (A-B; E) or 200 µM (C-D; F-H) of dAdo or dGuo were used to treat the cells. Apoptosis rates were analyzed 24 h post-treatment. Data are the mean (± standard deviation [SD]) values from three independent determinations. Statistically significant differences were analyzed with one-way analysis of variance (ANOVA) and Tukey's multiple-comparison test; ns, not significant ($P \geq 0.05$); *, $P < 0.05$; **, $P < 0.01$; ***, $P < 0.001$.

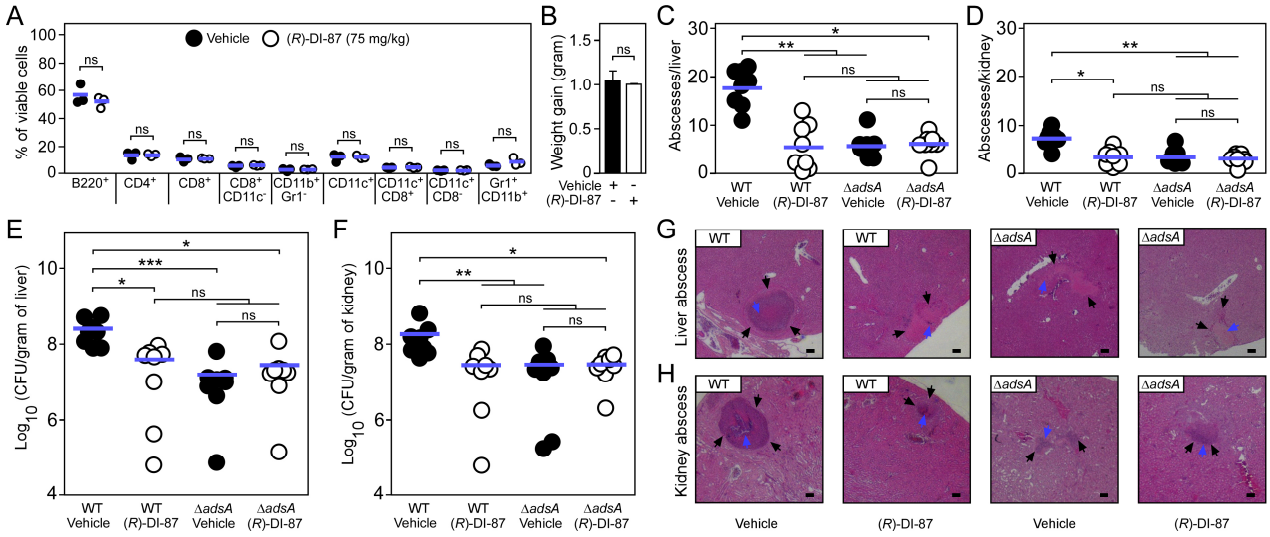

Figure 4. (*R*)-DI-87 protects against *S. aureus* invasive disease. (A, B) Safety assessment of (*R*)-DI-87 in mice. Cohorts of female C57BL/6 mice were treated with (*R*)-DI-87 (75 mg/kg) or vehicle (40% Captisol) via oral gavage in 12-hour intervals for 16 days. On day 16, peripheral blood was collected and subjected to a FACS-based immuno-phenotyping approach (A). Panel B indicates the body weight gain during the course of treatment. **(C-F)** Enumeration of visible surface abscesses and staphylococcal loads in organs of *S. aureus*-challenged C57BL/6 mice treated with (*R*)-DI-87 (75 mg/kg) or vehicle (40% Captisol). Mice received (*R*)-DI-87 (75 mg/kg) or vehicle (40% Captisol) via oral gavage every 12 hours and were challenged with 10^7 CFU of wild-type *S. aureus* Newman (WT) or its Δ*adsA* mutant. Data for female C57BL/6 mice are displayed ($n = 8$). Bacterial burden was enumerated as $\log_{10}$ CFU per gram of tissue at 5 days post-infection. Horizontal blue bars represent the mean values of visible abscesses per organ (C-D) or indicate the mean CFU count in each cohort (E-F). **(G, H)** Microscopic images of H&E–stained liver (G) or renal tissues (H) obtained after necropsy of *S. aureus*-challenged C57BL/6 mice treated with (*R*)-DI-87 (75 mg/kg) or vehicle (40% Captisol). Mice received (*R*)-DI-87 (75 mg/kg) or vehicle (40% Captisol) via oral gavage every 12 hours and were challenged with 10^7 CFU of wild-type *S. aureus* Newman (WT) or its Δ*adsA* mutant. Arrows point to immune cell infiltrates (black) or replicating staphylococci (blue). Black bars depict a length of 100 µm. Representative images are shown. Statistically significant differences were analyzed by a two-tailed Student's t-test (A-B) or with the Kruskal–Wallis test corrected with Dunn's multiple comparison (C-F). ns, not significant ($P > 0.05$); *, $P < 0.05$; **, $P < 0.01$; ***, $P < 0.001$.

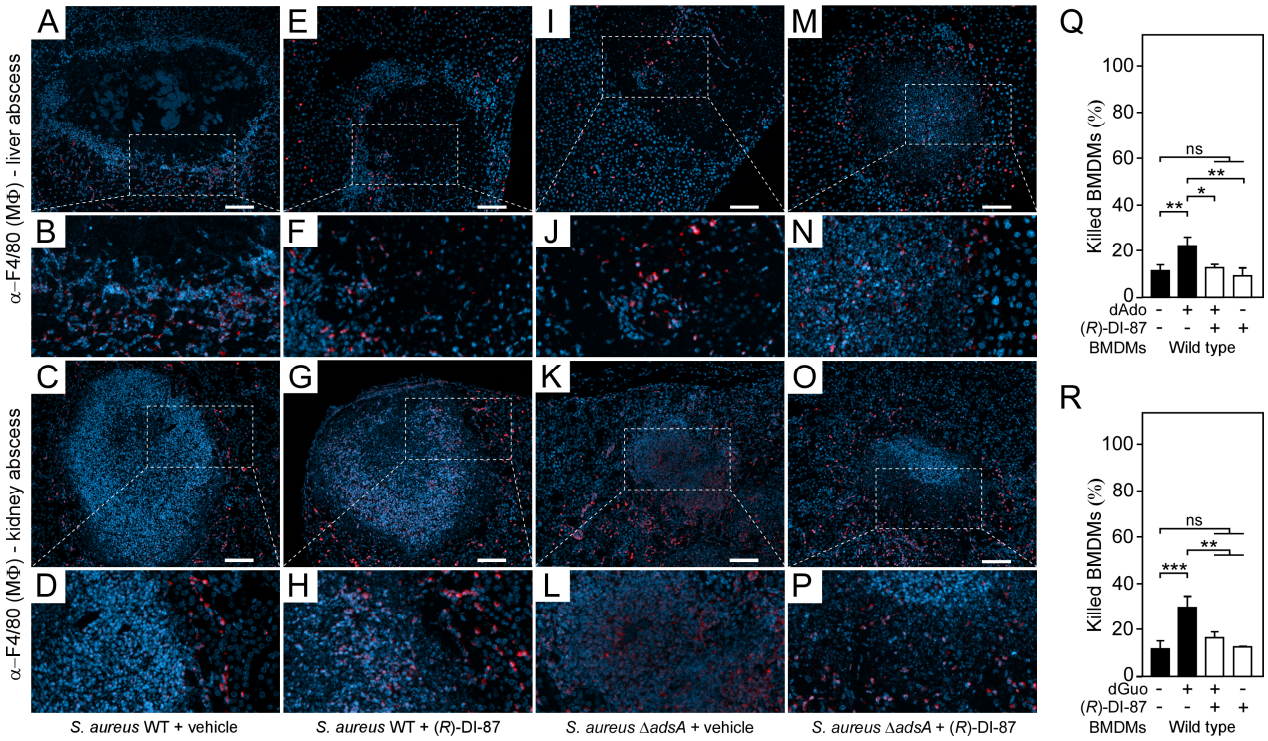

Figure 5. (*R*)-DI-87-mediated inhibition of dCK enhances macrophage infiltration into staphylococcal abscesses. (A-P) Immunofluorescence microscopy-based detection of macrophages in liver or renal tissues isolated 5 days after intravenous injection of 10^7 CFU of wild-type *S. aureus* Newman (A-H) or its *adsA* mutant (I-P) into wild type C57BL/6 mice treated with (*R*)-DI-87 (75 mg/kg) or vehicle (40% Captisol). Mice received (*R*)-DI-87 (75 mg/kg) or vehicle (40% Captisol) via oral gavage every 12 hours. Magnifications of boxed areas from upper panels are indicated. Thin sections were stained with α-F4/80 antibodies (macrophages; red). Nuclei were labeled with DAPI (blue). White bars shown in the upper panels depict 100 µm length. Representative images are shown. **(Q, R)** Survival rates of murine bone marrow-derived macrophages (BMDMs) exposed to dAdo (Q) or dGuo (R) in the presence (+) or absence (-) of 1 µM (*R*)-DI-87. Cells were also exposed to the inhibitor or vehicle only. 200 µM of dAdo or dGuo were used to treat the cells. Cell survival rates were analyzed 48 h post-treatment. Data are the mean (± standard deviation [SD]) values from three independent determinations. Statistically significant differences were analyzed with one-way analysis of variance (ANOVA) and Tukey's multiple-comparison test; ns, not significant ($P \geq 0.05$); *, $P < 0.05$; **, $P < 0.01$; ***, $P < 0.001$.

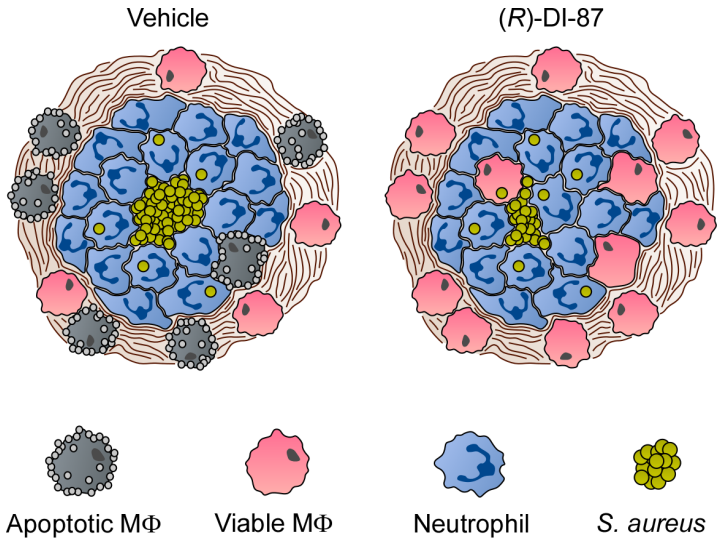

Figure 6. Proposed model of (*R*)-DI-87-mediated protection of phagocytes during *S. aureus* abscess formation. Diagram illustrating the (*R*)-DI-87-mediated protection of macrophages during the development of staphylococcal abscesses. While phagocytes get killed by *S. aureus*-derived death-effector deoxyribonucleosides in vehicle-treated animals, (*R*)-DI-87 protects macrophages and boosts their infiltration into the deeper cavity of infectious foci thereby enhancing eradication of staphylococci.